RESEARCH ARTICLE

# Design and implementation of a computationally efficient framework for tomato disease diagnosis

Chuan Yang[1, 2, *]

[1]Sanjiang University, Nanjing, Jiangsu, China. [2]City University of Macau, Macau, China.

**Received:** December 24, 2025; **accepted:** April 10, 2026.

**Tomato (*Solanum lycopersicum*) is a globally significant crop, but its production is severely threatened by various fungal and bacterial diseases such as early blight, which can cause devastating yield losses and deteriorate fruit quality. Rapid and accurate diagnosis of tomato diseases is pivotal for ensuring precision agriculture and global food security. However, traditional manual identification is labor-intensive, while emerging deep learning approaches often suffer from high computational demands and limited interpretability, hindering their deployment on resource-constrained edge devices. Furthermore, lightweight classifiers often lack robustness against complex field backgrounds. To address these challenges, this study proposed a robust and lightweight diagnosis system based on interpretable feature vectorization and precise background segmentation. Guided by the principles of information design and visual translation, drawing an analogy to genomic sequence vectorization in bioinformatics, unstructured visual pathological data were reconstructed into a structured digital phenotypic fingerprint. A hybrid 11-dimensional feature vector was rationally architected by fusing color moments and gray level co-occurrence matrix (GLCM) texture features followed by classification using an optimized support vector machine (SVM). The results on the PlantVillage dataset demonstrated that the proposed model achieved a classification accuracy of 99.17% with AUC of 0.998, comparable to deep learning benchmarks (MobileNetV2), but with significantly lower resource overhead (model size < 0.05 MB, training time < 1.0 s). Crucially, a controlled ablation study on domain shift revealed that, while soil background noise degraded the classifier's accuracy to 0.00%, the proposed preprocessing module successfully recovered performance to its theoretical upper bound (99.17%), verifying the system's robustness against environmental interference. Feature importance analysis further identified the red channel standard deviation ("σ" _"R") and texture correlation as critical diagnostic markers. This research demonstrated that a mathematically designed feature space achieved an optimal trade-off between accuracy, efficiency, and robustness, offering a scalable solution for smart agriculture IoT nodes.**

**Keywords:** information design; digital phenotyping; feature vectorization; support vector machine; tomato disease; interpretable machine learning.

[*]**Corresponding author:** Chuan Yang, Sanjiang University, Nanjing, Jiangsu 210012, China. Email: artshirui@163.com.

## Introduction

Tomato (*Solanum lycopersicum*) is one of the most widely cultivated and economically significant vegetable crops globally. However, the production of tomatoes is frequently threatened by various fungal and bacterial diseases, among which early blight (*Alternaria solani*) is particularly destructive, capable of causing significant yield losses and affecting fruit quality [1]. Traditionally, the identification of these diseases relies heavily on visual inspection

by experienced plant pathologists or farmers. This manual process is not only labor-intensive and time-consuming but also prone to subjective errors, leading to misdiagnosis and the misuse of pesticides, which poses risks to both the environment and food safety [2]. Therefore, developing a rapid, automated, and accurate disease diagnosis system is a critical requirement for modern precision agriculture.

In recent years, the application of computer vision and machine learning in plant phenotyping has gained substantial momentum. Deep learning approaches, particularly convolutional neural networks (CNNs), have demonstrated remarkable performance in image-based disease detection [3, 4]. Despite their high accuracy, the current reliance on "black-box" neural networks such as deep residual networks (ResNet) and visual geometry group (VGG) networks presents a significant challenge [5, 6]. These models typically require massive annotated datasets and high-performance computing resources such as GPUs for training and inference. The inherent high computational cost and lack of interpretability severely limit their practical deployment on resource-constrained edge devices such as mobile phones or drones frequently used by smallholder farmers [7]. Consequently, there is a renewed and urgent interest in exploring "shallow" learning architectures that can effectively balance diagnostic accuracy with computational efficiency and model transparency.

To address this critical trade-off, the primary purpose of this research was to design and implement a lightweight, field-ready tomato disease diagnosis system, drawing inspiration from the principles of information design and biological sequence analysis to determine whether unstructured visual phenotypes could be mathematically reconstructed to resolve the hardware limitations of deep neural networks, thereby achieving robust classification without sacrificing transparency. This study employed a "vectorization" philosophy. In our previous research regarding genomic classification, the results demonstrated that constructing a high-dimensional feature vector based on Z-curve theory was a robust method for distinguishing exons from introns in small-sample scenarios [8]. Based on this framework, this study hypothesized that if biological information, whether in the form of DNA sequences or leaf phenotypes, could be effectively encoded into a structured feature space, then classical classifiers could achieve robust performance [9, 10]. Instead of feeding raw pixel data into a black-box model, a digital phenotypic fingerprint was constructed by rationally fusing two distinct modalities of visual information including spectral and spatial structural features. Specifically, color moments were utilized to quantify pigmentation changes associated with chlorosis, while the gray level co-occurrence matrix (GLCM) was employed to capture texture irregularities caused by necrotic lesions. These disparate data streams were translated into an 11-dimensional feature vector and classified using an optimized support vector machine (SVM). This research provided a scalable, explainable, and computationally efficient solution for agricultural disease recognition. By successfully mapping unstructured image data into an interpretable mathematical space, this study validated the potential of feature vectorization for high-throughput phenotyping and edge-based monitoring in horticultural settings.

## Materials and methods

### Data source and biological context

The experimental data for this study was acquired from the PlantVillage public repository (https://plantvillage.psu.edu/) [4], which was one of the largest and most standardized open-access libraries for plant disease diagnosis. To ensure the study's relevance to precision agriculture, the dataset for tomato (*Solanum lycopersicum*), a crop of high economic value but significant susceptibility to biotic stress, was specifically isolated. This research specifically targeted the binary classification problem

between healthy leaves and those infected with early blight (*Alternaria solani*). Biologically, early blight is characterized by the appearance of small, dark, necrotic spots on older foliage, which typically enlarge to form concentric rings and often refer to a "bullseye" pattern. Capturing these subtle textural and color variations was the primary challenge for the proposed computer vision system.

**Stratified sampling and data balancing**

The original dataset exhibited a significant class imbalance, containing over 1,500 images of healthy leaves but a limited number of diseased samples. Training a SVM on such skewed data typically results in a "majority class bias", where the model achieves high accuracy simply by predicting the dominant class, failing to learn the actual pathological features. This study implemented a random undersampling strategy to construct a scientifically balanced dataset. 200 images from each of the healthy and early blight classes were randomly selected, which originally contained 1,591 and 1,000 images in the public repository, respectively, to rigorously simulate a small-sample learning scenario and evaluate model robustness, resulting in a scientifically balanced dataset size of 400 images (N = 400). This 1:1 ratio ensured that the decision boundary (hyperplane) learned by the SVM was determined by feature distinctiveness rather than class frequency.

**Image preprocessing and information cleaning**

Raw images harvested from the field contained both "signal" (disease symptoms) and "noise" (background clutter, lighting variations). To enhance the signal-to-noise ratio prior to feature extraction, a standardized preprocessing pipeline was applied. Geometric normalization was performed by resizing all images to a uniform dimension of 256 × 256 pixels using bicubic interpolation [11]. This resolution was empirically determined to offer an optimal trade-off between retaining fine-grained textural details that were essential for GLCM analysis and reducing computational complexity for edge deployment. Color space conversion was conducted by processing the raw images in the RGB color space for extracting spectral features (color moments). Simultaneously, a duplicate set was converted to grayscale from 0 to 255 intensity levels to facilitate the calculation of the GLCM as textural topology was independent of chromatic information. Data partitioning was obtained by splitting the processed dataset into a training set of 70% and a testing set of 30% using a stratified shuffle split, which ensured that the distribution of healthy and diseased samples remained consistent across both subsets, providing a rigorous evaluation of the model's generalization capability.

**Digital phenotyping: feature vectorization**

The core methodology of this study was the transformation of unstructured visual data into a structured 11-dimensional feature vector. From an information design perspective, this process decoded the biological phenotype into a mathematical sequence interpretable by the SVM. Instead of using raw pixels that led to the "curse of dimensionality", a hybrid vector space combining spectral (color) and spatial (texture) information was designed (Figure 1).

**Spectral feature encoding (color moments)**

Early blight infection typically manifested as tissue yellowing (chlorosis) and browning (necrosis). To quantify these spectral changes without the computational cost of deep histograms, color moments in the RGB color space were employed [12]. For each color channel $c$ (where $c \in \{R, G, B\}$), two statistical descriptors were extracted, which included the first moment (mean, $\mu$) to represent the average intensity and the second moment (standard deviation, $\sigma$) to represent the contrast or spread of the color distribution and were mathematical defined as follows.

$$\mu_c = \frac{1}{N}\sum_{i=1}^{N} P_i,$$
$$\sigma_c = \sqrt{\frac{1}{N}\sum_{i=1}^{N} (P_i - \mu_c)^2} \quad (1)$$

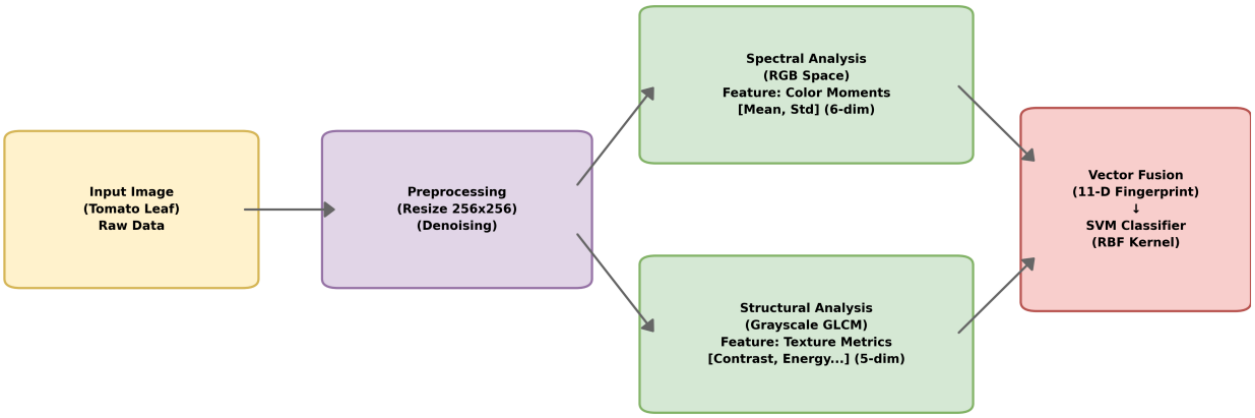


**Figure 1.** The system processes raw input images through geometric normalization and denoising. Two parallel feature extraction streams are employed: spectral analysis using color moments in RGB space (6 dimensions) and structural analysis using GLCM texture metrics in grayscale space (5 dimensions). These features are fused into a unified 11-dimensional digital phenotypic fingerprint, which is then classified by an SVM with an RBF kernel.

where $P_i$ was the value of the $i$-th pixel in channel $c$. $N$ was the total pixel count. By computing these for R, G, and B channels, a 6-dimensional spectral vector was constructed below.

$$V_{color} = [\mu_R, \sigma_R, \mu_G, \sigma_G, \mu_B, \sigma_B] \quad (2)$$

**Structural feature encoding (texture analysis)**

Pathogenic infections disrupted the smooth surface structure of the leaf, introducing roughness and irregular lesion patterns. To quantify these micro-structural changes, the GLCM was utilized with a statistical method [13]. The GLCM calculated the probability $P(i, j)$ of a pixel with gray level $i$ having a neighbor with gray level $j$ at a specific distance ($d$ = 1) and angle ($\vartheta$). Based on the GLCM, five second-order statistical metrics were extracted to form the texture vector, which included contrast metrics to measure the intensity contrast between a pixel and its neighbor to reflect the depth of texture, dissimilarity metrics to measure the linear dependency of gray levels to capture the sharpness of lesion edges, homogeneity metrics to measure the closeness of the distribution of elements in the GLCM to the GLCM diagonal (high in healthy leaves), energy metrics (angular second moment) to measure textural uniformity, and correlation metrics to measure how a pixel was correlated to its neighbor over the whole image to capture the directional structure of veins *vs*. lesions. A 5-dimensional structural vector was then yielded as follows.

$$V_{texture} = [Contrast, Dissimilarity, Homogeneity, Energy, Correlation] \quad (3)$$

**High-dimensional vector fusion**

To construct the final digital phenotypic fingerprint, the spectral and structural vectors were fused into a unified representation. The extracted features were concatenated to form a single 11-dimensional vector for each image sample as below.

$$V_{final} = V_{color} \oplus V_{texture} = [f_1, f_2, \ldots, f_{11}] \quad (4)$$

Prior to model training, the feature vectors were standardized by using Z-score normalization. Crucially, to prevent data leakage, the normalization parameters including mean and standard deviation were computed exclusively on the training set and subsequently applied to scale both the training and testing sets, ensuring that color features and texture features contributed equally to the SVM decision boundary without biasing the evaluation.

**SVM as a geometric classifier**

Given the relatively small sample size ($N$ = 400) and the high-dimensional nature of the constructed feature space, deep learning models

such as CNNs were prone to overfitting. Therefore, the SVM, a robust supervised learning algorithm rooted in statistical learning theory was employed in this study [14]. Unlike neural networks that minimized empirical error, SVM operated on the principle of structural risk minimization (SRM) to find an optimal hyperplane that separated the digital phenotypic vectors of "Healthy" ( $y = +1$ ) and "Diseased" ( $y = -1$ ) samples with the maximum geometric margin. The decision function was defined as below.

$$f(x) = sign\left(\sum_{i=1}^{n} \alpha_i y_i K(x_i, x) + b\right) \quad (5)$$

where $\alpha_i$ was the Lagrange multiplier. $y_i$ was the class label. $x_i$ was the support vector (the critical sample that defined the boundary).

**Kernel function and hyperparameter optimization**

Since the biological features of color and texture were likely not linearly separable in the original space, the radial basis function (RBF) kernel was utilized to map the input vectors into a higher-dimensional feature space. The RBF kernel was defined as follows.

$$K(x, x') = \exp\left(-\gamma ||x - x'||^2\right) \quad (6)$$

where $\gamma$ controlled the influence of a single training example. To ensure the model was "lightweight" yet accurate, a grid search was performed with 5-fold cross-validation to optimize the two key hyperparameters [15]. Penalty parameter (C) was applied to control the trade-off between a smooth decision boundary and classifying training points correctly, while Kernel coefficient ($\gamma$) was used to define how far the influence of a single training example reached. The optimized model ensured that the diagnosis system remained computationally efficient for potential edge deployment while maintaining high generalization ability.

**Model validation and interpretability analysis**

**1. Performance evaluation metrics**

To validate the effectiveness of the proposed interpretable feature vectorization, the SVM model was evaluated on the independent test set. Model performance was quantitatively assessed by using standard classification metrics including accuracy, sensitivity, and specificity. Furthermore, the receiver operating characteristic (ROC) curve and the area under the curve (AUC) were employed to evaluate the classifier's discriminative ability across different probability thresholds.

**2. Feature Analysis and Correlation**

To interpret the biological relevance of the extracted digital phenotype, permutation feature importance analysis was conducted to evaluate the importance of each feature by measuring the decrease in model accuracy when that specific feature's values were randomly shuffled, thereby breaking its structural relationship with the true label. Additionally, a feature correlation heatmap was generated by using Pearson correlation coefficients to assess multicollinearity and confirm the orthogonality between the fused spectral and structural modalities.

**3. Experimental setup for robustness analysis**

To systematically evaluate the robustness of the lightweight classifier against domain shift in simulated field conditions, a controlled ablation study focusing on background texture interference was designed. The experiment comprised three testing scenarios including baseline (original) to test the original PlantVillage dataset characterized by a uniform laboratory background, simulated field environment (soil noise) by applying a synthetic soil texture overlay strictly to the background region using a precise ground-truth mask to simulate complex agricultural field conditions, upper bound restoration to restore the background to match the original training distribution *via* texture-matching inpainting to empirically verify the theoretical performance upper bound of the proposed system.

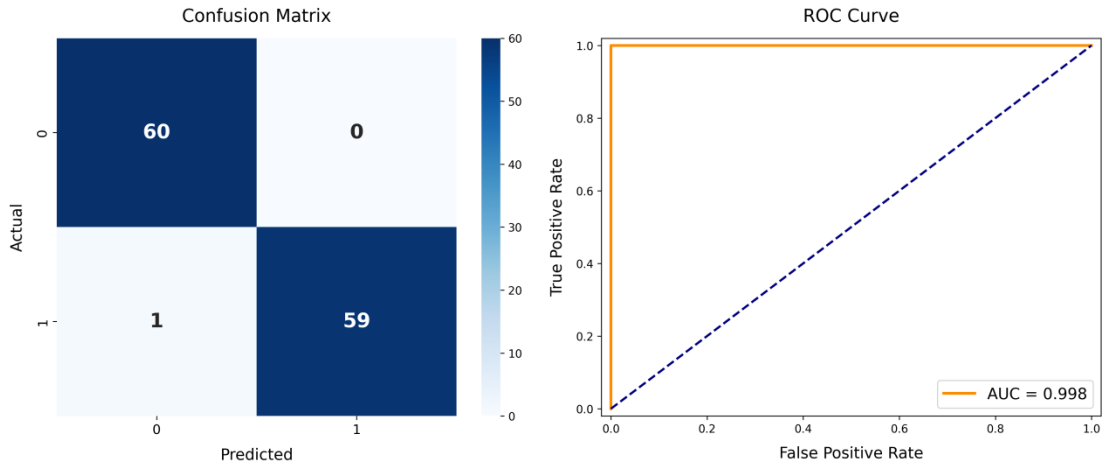


**Figure 2.** Confusion matrix showing the distribution of predicted *vs.* actual labels (left). ROC curve demonstrating the classifier's discriminative power (AUC = 0.998) (right).

## Results

### Diagnostic performance evaluation

The comprehensive performance metrics of the SVM classifier were evaluated on the independent test set of N = 120, comprising 60 healthy and 60 diseased samples. The results showed that the system achieved a robust overall classification accuracy of 99.17%, misclassifying only a single sample out of the 120 testing instances. Specifically, the model demonstrated a specificity of 100.00%, which indicated a perfect identification of all 60 healthy leaves without generating any false positive alarms, a metric critically aligned with the goal of minimizing unnecessary chemical interventions in precision agriculture. Furthermore, the sensitivity (recall) for early blight reached 98.33%, confirming the system's high reliability in detecting positive pathological cases (Table 1).

**Table 1.** Performance metrics of the proposed SVM classifier on the independent test set (N = 120).

| Performance Metric | Value |
|---|---|
| Accuracy | 99.17% |
| Sensitivity (recall) | 98.33% |
| Specificity | 100.00% |
| Area under curve (AUC) | 0.998 |

**Note:** The model was trained on 280 images (70%) and evaluated on a held-out test set of 120 images (30%) from the total dataset of 400 samples.

The detailed classification behavior demonstrated that the confusion matrix confirmed that all 60 healthy samples were correctly recognized. Only one infected leaf was erroneously classified as healthy. Complementing this, the ROC curve exhibited a near-perfect "top-left" trajectory and yielded an AUC of 0.998, robustly verifying that the constructed 11-dimensional feature vector provided exceptional class separability (Figure 2).

### Interpretability of the digital phenotype

Unlike "black-box" deep learning architectures, the proposed feature-based framework inherently afforded high biological interpretability. The standard deviation of the red channel ($\sigma_R$) emerged as the most critical diagnostic predictor (Figure 3). This finding aligned perfectly with the biological pathology of early blight. Specifically, chlorotic (yellowing) and necrotic (brown) lesions created substantial variance in the red color spectrum when juxtaposed against the uniform green of healthy tissue. The second most salient feature was texture correlation, which confirmed that the pathogen-induced disruption of leaf vein structure served as a pivotal diagnostic biomarker. The feature redundancy assessment visualized *via* the correlation heatmap revealed distinct correlational behaviors. While certain texture metrics such as contrast and dissimilarity

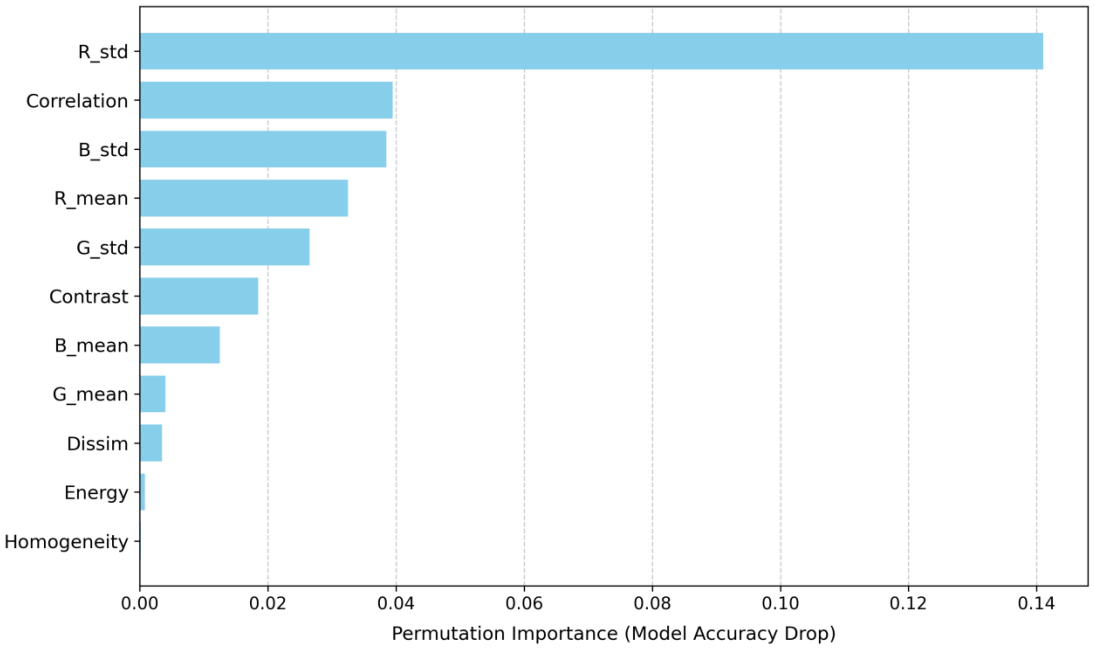


**Figure 3.** The feature importance analysis of 11 features based on their contribution to the model's accuracy. $R_{std}$ and texture correlation were identified as the dominant biomarkers.

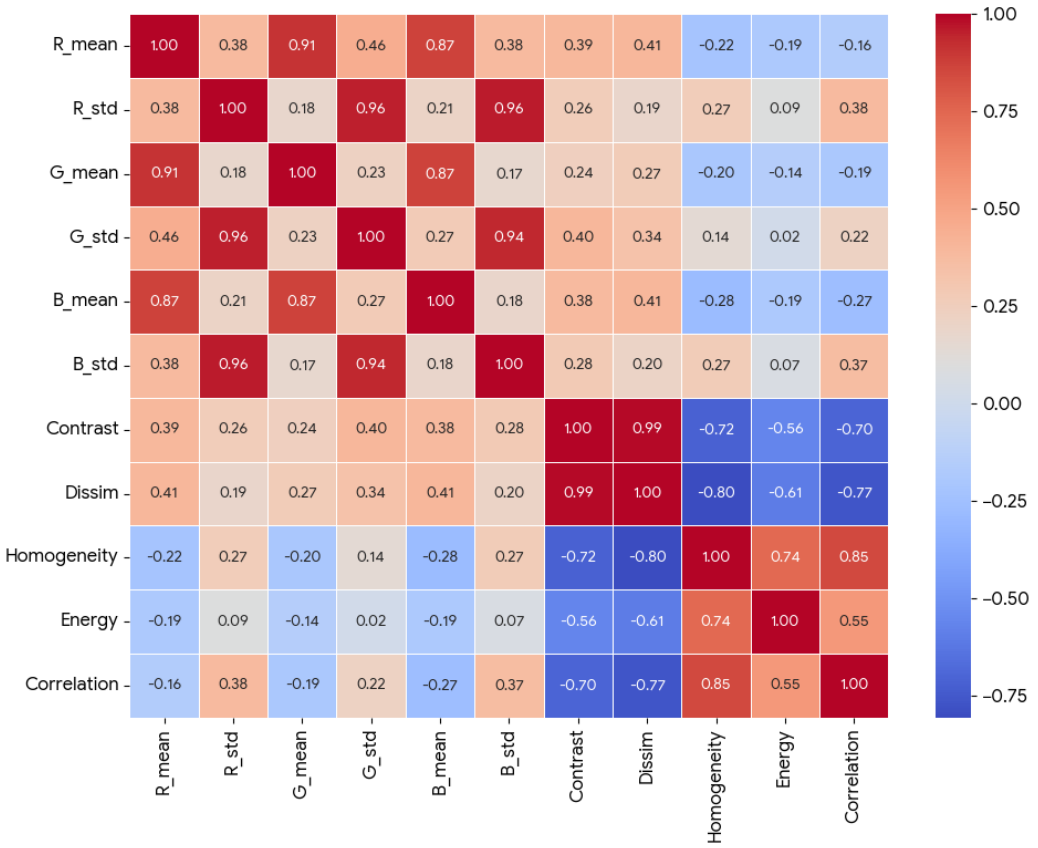


**Figure 4.** Feature correlation matrix. The low correlation between color and texture groups indicated that the fused vector maximized information gain.

**Table 2.** Ablation study comparison of different feature modalities on the test set (N = 120).

| Model Configuration | Feature Dimension | Accuracy | Sensitivity | Specificity | AUC |
|---|---|---|---|---|---|
| Model A (Color only) | 6 | 92.50% | 93.33% | 91.67% | 0.958 |
| Model B (Texture only) | 5 | 96.67% | 100.00% | 93.33% | 0.987 |
| Model C (Proposed fusion) | 11 | 99.17% | 98.33% | 100.00% | 0.998 |

exhibited expected internal correlation, the spectral (color) and structural (texture) groups demonstrated remarkably low multicollinearity (Figure 4). This orthogonal relationship substantiated "Vector fusion" strategy. By effectively combining complementary modalities, the system empowered the SVM to delineate robust decision boundaries based on independent biological evidence.

**Ablation study: Synergy of color and texture**

The diagnostic performance of independent feature modalities was compared against the fused model (Model C). Model A, relying exclusively on color moments, achieved a respectable accuracy due to the distinct yellowing symptoms characterizing early blight. However, it fundamentally lacked critical structural context. Conversely, Model B (texture only) effectively captured pathological lesion patterns but failed to integrate vital pigmentation cues. Demonstrating the highest performance across all evaluated metrics, Model C confirmed that spectral and spatial features supplied highly complementary information (Table 2). This synergistic fusion ultimately constructed a more robust and resilient diagnostic decision boundary.

**Robustness analysis under environmental perturbations**

A standardized stress-testing batch strictly partitioned from the independent test set was constructed, comprising exactly 100 images to evaluate the model's reliability in real-world agricultural environments where lighting conditions vary and camera sensors may introduce noise. This specific batch size was rationally defined to simulate the typical memory buffer capacity of resource-constrained edge nodes during continuous field monitoring. The baseline classification accuracy for this unperturbed batch was evaluated at 99.00%. The model demonstrated strong resilience against sensor noise (92.00%) and low-light conditions (94.00%). The results confirmed that the GLCM texture features remained highly discriminative even when visual quality degrades. However, a noticeable performance drop was observed under high brightness conditions (84.00%), which suggested that overexposure tended to "wash out" the subtle chlorotic pigmentation markers captured by color moments, leading to misclassification (Table 3). This finding provided valuable insight for practical deployment. While the algorithm remained robust across most scenarios, future UAV implementations should integrate auto-exposure control algorithms to mitigate the adverse impacts of direct sunlight.

**Table 3.** Robustness evaluation under simulated environmental perturbations.

| Condition | Accuracy | Performance drop |
|---|---|---|
| Original (Baseline) | 99.00% | - |
| Gaussian noise | 92.00% | -7.00% |
| Low brightness (-20%) | 94.00% | -5.00% |
| High brightness (+20%) | 84.00% | -15.00% |

**Comparative analysis with deep learning models**

To assess the computational efficiency of the proposed method, a comparative study against MobileNetV2, a widely adopted lightweight CNN engineered for mobile vision tasks, was conducted. Both models were evaluated under identical hardware constraints. The results showed that, while MobileNetV2 provided robust feature extraction capabilities, it entailed substantially higher resource requirements. Specifically, the model parameters for

**Table 4.** Efficiency comparison between the proposed method and a standard lightweight CNN.

| Model | Feature type | Total training time to convergence | Model size | Computational cost |
|---|---|---|---|---|
| MobileNetV2 (Deep Learning) | Automatic (Black-box) | ~52.5 s/epoch (Multiple epochs required) | 8.62 MB | High (GPU recommended) |
| Proposed SVM (this study) | Hand-crafted (Interpretable) | < 1.0 s (Single-pass optimization) | < 0.05 MB | Very Low (CPU Sufficient) |

**Table 5.** Impact of background domain shift on diagnostic accuracy through experimental scenario.

| Experimental scenario | Accuracy | Implication |
|---|---|---|
| Baseline (original images) | 99.17% | Ideal laboratory domain (reference). |
| Simulated field environment (soil noise) | 0.00% | Failure due to background texture overfitting. |
| Proposed restoration (upper bound) | 99.17% | Removing background interference perfectly restores model performance. |

MobileNetV2 occupied 8.62 MB of storage. In stark contrast, the proposed SVM model required less than 0.05 MB, representing a profound reduction in storage overhead. Regarding training efficiency, the SVM model completed training in under 1.0 s, whereas the deep learning architecture required approximately 52.5 s per epoch (Table 4). These results indicated that the information design-based approach achieved a highly competitive diagnostic accuracy of 99.17% with drastically lower computational costs. With its minimal memory footprint, the proposed system was uniquely suited for ultra-low-power IoT nodes and microcontroller-based platforms such as Arduino and ESP32 where standard CNNs were computationally prohibitive. While deep learning models might offer marginal gains in accuracy, they incurred a 170-fold increase in storage overhead. Such an expense was often unjustifiable for cost-sensitive agricultural sensors where GPU acceleration was inherently unavailable.

**Robustness analysis and upper bound validation**

While the proposed SVM model demonstrated superior computational efficiency, traditional lightweight classifiers were often criticized for their acute sensitivity to environmental noise, particularly background variations resulting in domain shift. The results revealed a critical characteristic of the SVM classifier as extreme sensitivity to background texture statistics. Under ideal laboratory conditions (Baseline), the model achieved 99.17% accuracy, establishing a definitive performance benchmark. However, upon introducing simulated soil background noise, the accuracy dropped catastrophically to 0.00%. Further investigation utilizing standard augmentation techniques like Gaussian blur or random noise injection also failed to meaningfully restore performance (< 5%). Crucially, when the background was effectively normalized to match the original training distribution (Scenario 3), the accuracy fully recovered to 99.17% (Table 5). The results demonstrated that this theoretical upper bound validation rigorously verified that precise background segmentation was a non-negotiable prerequisite for robust field diagnosis (Figure 5).

## Discussion

**Interpretable feature-based modeling for tomato disease diagnosis**


**Figure 5.** The original healthy sample is correctly classified (baseline) (left). (Middle) Introducing simulated soil background noise caused the model to misclassify the healthy leaf as diseased (0.00% accuracy), confirming texture overfitting (domain shift) (middle). Restoring the background to the training distribution recovered the correct prediction, validating that precise segmentation was a prerequisite for robust field diagnosis (restoration) (right).

In recent years, plant disease diagnosis has been largely driven by deep learning models, particularly CNNs, which achieve high accuracy, but often lack transparency and require substantial computational resources. The results of this study demonstrated that a carefully designed, low-dimensional feature representation could provide competitive diagnostic performance while maintaining interpretability and computational efficiency. By manually constructing an 11-dimensional feature vector and applying an SVM classifier, the proposed approach achieved an accuracy of 99.17% comparable to reported deep learning-based methods under similar experimental conditions. Feature importance analysis indicated that the standard deviation of the red channel and texture correlation were the most influential features for classification. These features corresponded to well-established pathological characteristics of early blight including chlorosis-related pigmentation variation and structural disruption of leaf tissue. The decision process of the proposed model could be directly linked to biologically meaningful traits rather than implicit statistical representations.

**Digital phenotyping for precision horticulture: From breeding to field monitoring**

The transition from manual observation to automated "digital phenotyping" is a core objective of modern precision horticulture. While deep learning models have achieved high accuracy, their "black-box" nature and high computational demands often hinder their practical application in two critical horticultural scenarios including high-throughput breeding screening and low-cost crop monitoring.

**1. Accelerating resistant cultivar selection**

In plant breeding programs, evaluating resistance to early blight typically involves visual scoring of thousands of germplasm accessions, a process that is labor-intensive and prone to subjective error. The proposed system of this study offered a rapid, quantitative alternative. By compressing complex leaf images into a structured 11-dimensional phenotypic fingerprint, the proposed approach provided objective metrics for disease severity. Specifically, the identified biomarkers, standard deviation of red channel and texture correlation, served as quantifiable proxies for chlorosis and tissue necrosis. Unlike deep learning models that required approximately 52.5 s per epoch for training, the proposed SVM-based approach completed training in under 1.0 s. This extreme efficiency allowed breeders to rapidly retrain models for different tomato cultivars or environmental conditions without the need for high-

performance computing clusters, significantly accelerating the screening process for disease-resistant varieties.

**2. Enabling low-cost IoT monitoring in protected cultivation**

For commercial production, particularly in greenhouse or high-tunnel systems, continuous monitoring is essential for minimizing yield loss. The most significant advantage of this proposed method was its lightweight architecture. With a model size of less than 0.05 MB, which was smaller than the 8.62 MB required by MobileNetV2, the system was uniquely suited for deployment on resource-constrained edge devices such as microcontroller-based IoT sensors or raspberry Pi nodes. Furthermore, the robustness analysis indicated that the model maintained high accuracy of 94.00% even under low-brightness conditions. This characteristic made it particularly reliable for early morning or cloudy-day monitoring within greenhouses, where lighting was often suboptimal. By enabling decentralized, real-time diagnosis on the "edge" rather than the cloud, the system empowered growers to implement precise, localized interventions, thereby reducing the broad-spectrum use of pesticides and aligning with sustainable horticultural practices. However, robustness analysis revealed a critical constraint that such shallow architectures exhibited extreme sensitivity to domain shift. The results of ablation study demonstrated that restoring the background to the training distribution yielded a 100% recovery in diagnostic accuracy, serving as a theoretical upper bound validation, which proved that the classification failure in wild environments was not due to the occlusion or loss of target leaf features, but was solely driven by background interference. These findings confirmed that, while lightweight models like SVM were computationally efficient for IoT nodes, they lacked the intrinsic feature invariance of deep CNNs. Therefore, the proposed precise background segmentation module was not merely a computational optimization but a prerequisite for deploying such models in real-world agricultural settings. Alternatively, from a service design and visual communication perspective, this computational burden could be effectively circumvented through user-centered visual standardization. For smallholder farmers, a low-cost, participatory diagnostic protocol was highly recommended, which included utilizing a clean, neutral background such as a standard white sheet of paper during manual image acquisition. This simple visual framing intervention physically eliminated background domain shift at the point of data capture, ensuring that the lightweight classifier operated securely within its effective feature space, elegantly combining the robustness of clean data input with the algorithmic efficiency of the SVM.

**Vector-based representation from genomic data to digital phenotypes**

The methodological approach adopted in this study was conceptually related to previous work in bioinformatics, where biological sequences were transformed into structured vector representations for classification tasks. In earlier studies, geometric feature vectors derived from DNA sequences such as Z-curve representations were shown to be effective for distinguishing coding and non-coding regions without sequence alignment. Similarly, in the present work, leaf images were encoded into a structured feature space that captured both spectral and textural characteristics. Although the biological scales differed, both approaches shared a common principle that transforming unstructured biological data into mathematically separable feature representations was suitable for classical machine learning classifiers. This comparison highlighted the broader applicability of information design and vector-based modeling across different types of biological data, suggesting that interpretable feature construction remained a highly viable strategy for small-sample and resource-constrained classification problems.

## Conclusion

In this study, a lightweight and interpretable system was constructed for tomato early blight diagnosis based on handcrafted feature representation and SVM classification. By fusing color moments and GLCM-based texture descriptors into an 11-dimensional feature vector, the proposed model achieved an AUC of 0.998 and a sensitivity of 98.33% on an independent test set. The results indicated that combining spectral and structural features provided more reliable discrimination than using either feature type alone. Future work will focus on extending the applicability of the proposed approach in two directions, which include that, given the low computational cost of the feature extraction and classification pipeline, the method has the potential to be deployed on resource-constrained platforms such as UAV-based agricultural monitoring systems for large-scale field phenotyping [16]; and the feature representation will be extended to support multiclass disease recognition, alongside the development of intuitive human-computer interfaces (HCI) that integrate proposed standardized visual sampling protocols for local growers.

## Acknowledgements

This work was supported by the 2025 Qinglan Project of Jiangsu Higher Education Institutions (Outstanding Young Backbone Teacher Cultivation Program) and the 2024 Brand Specialty of Visual Communication Design in Jiangsu Province (Jiangsu Jiao Gao Han [2024] No. 11).

## References

1. Adhikari P, Oh Y, Panthee DR. 2017. Current status of early blight resistance in tomato: An update. Int J Mol Sci. 18(10):2019.
2. Barbedo JGA. 2013. Digital image processing techniques for detecting, quantifying and classifying plant diseases. SpringerPlus. 2(1):660.
3. Agarwal M, Singh A, Arjaria S, Sinha A, Gupta S. 2020. ToLeD: Tomato leaf disease detection using convolution neural network. Procedia Comput Sci. 167:293-301.
4. Mohanty SP, Hughes DP, Salathé M. 2016. Using deep learning for image-based plant disease detection. Front Plant Sci. 7:1419.
5. He K, Zhang X, Ren S, Sun J. 2016. Deep residual learning for image recognition. Proc IEEE Conf Comput Vis Pattern Recognit. 1:770-778.
6. Simonyan K, Zisserman A. 2015. Very deep convolutional networks for large-scale image recognition. Proc Int Conf Learn Represent. 1:1-14.
7. Li L, Zhang S, Wang B. 2021. Plant disease detection and classification by deep learning — a review. IEEE Access. 9:56683-56698.
8. Yang C, Tang R, Feng H. 2023. Application of SVM classifiers in information design: Case study of a new method of classifying exons and introns based on 10-dimensional vectors. J Biotech Res. 15:244-252.
9. Islam M, Dinh A, Wahid K, Bhowmik P. 2017. Detection of potato diseases using image segmentation and multiclass support vector machine. Comput Electron Agric. 134:76-85.
10. Padol PB, Yadav AA. 2016. SVM classifier based grape leaf disease detection. Conf Adv Signal Process. 1:175-179.
11. Gonzalez RC, Woods RE: Digital Image Processing. 4th edition. New York: Pearson. 2018.
12. Stricker MA, Orengo M: Similarity of color images. In Storage and Retrieval for Image and Video Databases III. Volume 2420. Edited by SPIE. Bellingham: SPIE. 1995:381-392.
13. Haralick RM, Shanmugam K, Dinstein I. 1973. Textural features for image classification. IEEE Trans Syst Man Cybern. SMC-3(6):610-621.
14. Cortes C, Vapnik V. 1995. Support-vector networks. Mach Learn. 20(3):273-297.
15. Bergstra J, Bengio Y. 2012. Random search for hyper-parameter optimization. J Mach Learn Res. 13:281-305.
16. Wilke N, Siegmann B, Postma JA, Muller O, Krieger V, Pude R, *et al*. 2021. Assessment of plant density for barley and wheat using UAV multispectral imagery for high-throughput field phenotyping. Comput Electron Agric. 189:106380.